The biotin-ligating protein BPL-1 is critical for lipid biosynthesis and polarization of the *Caenorhabditis elegans* embryo

Received for publication, May 23, 2017, and in revised form, November 16, 2017 Published, Papers in Press, November 20, 2017, DOI 10.1074/jbc.M117.798553

Jason S. Watts[‡], **Diane G. Morton**[§], **Kenneth J. Kemphues**[§], **and Jennifer L. Watts**[‡1]

From the [‡]*School of Molecular Biosciences and Center for Reproductive Biology, Washington State University, Pullman, Washington 99164-7520 and the* [§]*Department of Molecular Biology and Genetics, Cornell University, Ithaca, New York 14850*

Edited by George M. Carman

Biotin is an essential cofactor for multiple metabolic reactions catalyzed by carboxylases. Biotin is covalently linked to apoproteins by holocarboxylase synthetase (HCS). Accordingly, some mutations in HCS cause holocarboxylase deficiency, a rare metabolic disorder that can be life-threatening if left untreated. However, the long-term effects of HCS deficiency are poorly understood. Here, we report our investigations of *bpl-1*, which encodes the *Caenorhabditis elegans* ortholog of HCS. We found that mutations in the biotin-binding region of *bpl-1* are maternal-effect lethal and cause defects in embryonic polarity establishment, meiosis, and the integrity of the eggshell permeability barrier. We confirmed that BPL-1 biotinylates four carboxylase enzymes, and we demonstrate that BPL-1 is required for efficient *de novo* fatty acid biosynthesis. We also show that the lack of larval growth defects as well as nearly normal fatty acid composition in young adult worms is due to sufficient fatty acid precursors provided by dietary bacteria. However, BPL-1 disruption strongly decreased levels of polyunsaturated fatty acids in embryos produced by *bpl-1* mutant hermaphrodites, revealing a critical role for BPL-1 in lipid biosynthesis during embryogenesis and demonstrating that dietary fatty acids and lipid precursors are not adequate to support early embryogenesis in the absence of BPL-1. Our findings highlight that studying BPL-1 function in *C. elegans* could help dissect the roles of this important metabolic enzyme under different environmental and dietary conditions.

Biotin is an essential B vitamin that acts as a critical cofactor in metabolic reactions. Animals cannot synthesize biotin but rather must obtain biotin from plant or bacterial sources. In humans, biotin deficiency is rare because it is available from numerous dietary sources and synthesized by gut microbes (1). However, biotin deficiency does occur rarely in individuals who consume raw egg whites or who are fed parenteral diets without biotin, leading to hair loss, dermatitis, skin rash, ataxia, and neurologic dysfunction. Additionally, subclinical biotin deficiency was shown to be common during pregnancy, a condition that in mice prohibits normal fetal development (2).

Biotin functions primarily as a cofactor in carboxylation reactions. In mammals, five biotin-dependent carboxylases perform diverse metabolic functions in lipid synthesis, gluconeogenesis, amino acid catabolism, and odd-chain fatty acid oxidation. Biotin is covalently attached to carboxylase enzymes by the action of holocarboxylase synthetase (HCS),[2] a biotin-ligating protein (1, 3). In humans, mutations in the holocarboxylase synthetase gene result in a disease called holocarboxlase synthetase deficiency, or multiple carboxylase deficiency (MCD) (4, 5). The symptoms of MCD are phenotypically similar to biotin deficiency and present during infancy. If left untreated, MCD can cause coma and death. The underlying mutations causing holocarboxlase synthetase deficiency are well-documented, and the disease can be treated with large doses of biotin in most cases (6). However, the long-term effects of perturbing multiple metabolic pathways in these patients are poorly understood.

The nematode *Caenorhabditis elegans* offers a powerful model for studying complex metabolic systems. The invertebrate is amenable to forward and reverse genetics, has a short life cycle, and produces large numbers of offspring with well-characterized developmental processes that can be easily studied with light microscopy. Additionally, the *C. elegans* genome contains many orthologs to mammalian metabolic enzymes. These enzymes include orthologs to carboxylase enzymes and holocarboxlase synthetase, which previously were uncharacterized in *C. elegans*.

In a forward genetic screen, we obtained two mutations in a biotin ligase orthologous to mammalian holocarboxylase synthetase. These mutations cause maternal-effect embryonic lethality, demonstrating a key role for HCS in embryonic development. We show that BPL-1 biotinylates four key carboxylase enzymes, including acetyl-CoA carboxylase (ACC/POD-2), which is critical for maintaining the levels of embryonic polyunsaturated fatty acids and for the formation of the permeability barrier in the newly formed zygote. In the absence of BPL-1,

This work was supported by National Institutes of Health Grants T32GM083864 (to J. S. W.), R01DK074114 (to J. L. W.), and R01GM079112 and R01HD27689 (to K. J. K.). The authors declare that they have no conflicts of interest with the contents of this article. The content is solely the responsibility of the authors and does not necessarily represent the official views of the National Institutes of Health.

This article contains Movies S1–S3.

[1] To whom correspondence should be addressed: School of Molecular Biosciences, Washington State University, Pullman, WA 99164-7520. Tel.: 509-335-8554; E-mail: jwatts@vetmed.wsu.edu.

[2] The abbreviations used are: HCS, holocarboxylase synthetase; MCD, multiple carboxylase deficiency; PUFA, polyunsaturated fatty acid; ACC, acetyl-CoA carboxylase; NGM, nematode growth medium.

ACC/POD-2, and fatty acid desaturation, embryos fail to complete meiosis and fail to establish proper polarity during the first zygotic cell divisions. Unlike ACC/POD-2 deficiency, BPL-1 activity is dispensable during larval growth and development, because *C. elegans* are able to utilize fatty acid precursors from their bacterial diet. Our findings suggest that dietary precursors are partitioned away from embryonic lipids, and thus *de novo* lipid machinery is critical for the first steps of embryogenesis.

Results

mel-3 mutations correspond to the holocarboxylase synthetase gene

Mutations that defined the *mel-3* gene of *C. elegans* were first identified in a screen for maternal-effect lethal mutants. The *mel-3* mutations resulted in 100% lethality in embryos produced by homozygous mutant mothers and mapped to a region of linkage group II uncovered by the *mnDf30* deletion (7). Further mapping using deletion strains combined with complementation analysis and transformation rescue allowed us to identify a 7.5-kb BamHI fragment containing a single predicted gene, F13H8.10, that was capable of rescuing the embryo lethality of *mel-3(b281)* and *mel-3(it8).*

The F13H8.10 gene encodes a biotin protein ligase, homologous to the enzyme HCS, which is responsible for attaching biotin to carboxylases. For the remainder of this work, the *mel-3* gene will be referred to as *bpl-1*, biotin protein ligase-1. Sequence analysis of *b281* and *it8* mutants revealed point mutations in the coding sequence of F13H8.10 that result in single amino acid substitutions in the predicted protein product. These mutations affect amino acids within the biotin protein ligase catalytic domain that are highly conserved among all holocarboxylase synthetase genes (8). The *b281* mutation causes an A730E amino acid change, and *it8* results in G912D substitution in BPL-1 (Fig. 1*A*). Many human mutations of HCS resulting in multiple carboxylase deficiency disease have also been found in this region (6, 9). The *bpl-1* deletion alleles *tm5867* and *tm6621* remove portions of the conserved biotin protein ligase domain and are predicted to result in frameshift and early termination (Fig. 1*A*). These deletion mutations also result in 100% maternal-effect lethality ($n > 5000$ for each allele).

BPL-1 is essential for early embryonic development in C. elegans

Our phenotypic studies demonstrate that *bpl-1* plays an essential role in early embryonic development. 100% of embryos produced by homozygous mutant *bpl-1* worms fail to hatch. We used time-lapse video microscopy to compare early embryogenesis in *bpl-1* mutants with wild type. In wild-type *C. elegans*, the one-cell embryo divides asymmetrically to produce two daughter cells, AB and P1, which undergo asynchronous second divisions. First, the AB cell divides with a spindle orientation perpendicular to the anterior–posterior axis, followed by division of the P1 cell along the anterior–posterior axis (10). In contrast, *bpl-1* embryos show abnormal early division patterns, including synchronous and symmetrical divisions and abnormal spindle orientations (Fig. 1*B*, Table 1 and Movies S1–S3).

We found that 100% of two-cell stage *bpl-1* embryos are permeable to FM4-64 dye, indicating improper formation of the eggshell permeability barrier (Fig. 1*C*; $n = 45$). Embryos also display aneuploidy due to earlier meiotic defects (Fig. 1*C*). We observed extra nuclei in one-cell and two-cell embryos, consistent with failure of meiosis in 90% of *bpl-1* embryos (Table 1).

PAR (partitioning-defective) proteins are ancient, conserved proteins that localize asymmetrically and regulate cell polarity (10). We found that *bpl-1* embryos fail to segregate PAR proteins properly (Fig. 1*D*). Specifically, the posterior PAR-2 domain is severely restricted, whereas the anterior PAR-6/PAR-3/PKC-3 domain extends further into the posterior of the embryo. Like *b281* and *it8*, the deletion mutants *tm5867* and *tm6621* show the same range of embryo phenotypes, with the same penetrance (Table 1). *bpl-1* embryos do not undergo morphogenesis but arrest as a mass of many cells.

BPL-1 biotinylates carboxylase enzymes

The predicted amino acid sequence of BPL-1 is orthologous to holocarboxylase synthetase, which in mammals covalently links biotin to multiple carboxylase enzymes, including acetyl-CoA carboxylases 1 and 2, pyruvate carboxylase, 3-methylcrotonyl-CoA carboxylase, and propionyl-CoA carboxylase. These carboxylase enzymes function in a diverse set of metabolic pathways. Both the cytoplasmic acetyl-CoA carboxylase 1 and the mitochondrial acetyl-CoA carboxylase 2 catalyze the rate-limiting step in *de novo* fatty acid synthesis. Pyruvate carboxylase converts pyruvate to oxaloacetate in gluconeogenesis. Both 3-methylcrotonyl-CoA carboxylase and propionyl-CoA carboxylase are involved in catabolism of branched-chain amino acids, and propionyl-CoA carboxylase also functions in odd-chain fatty acid catabolism.

To determine whether BPL-1 biotinylates carboxylase enzymes in *C. elegans*, we probed total protein blots with streptavidin-horseradish peroxidase conjugates. Blots of proteins from wild-type control worms display prominent protein bands at ~240 and 130 kDa and two at ~70 kDa (Fig. 2*A*). The intensity of each of these bands is reduced in *bpl-1(b281)* homozygous adult worms, indicating a reduction in biotinylation of the proteins. To determine whether the biotinylated protein bands correspond to carboxylase enzymes, we knocked down *pod-2*, *pyc-1*, *pcca-1*, and *mccc-1* with RNAi.

The *pod-2* gene is predicted to encode acetyl-CoA carboxylase isoforms of 91.4, 230.6, and 242.6 kDa. When we knocked down *pod-2* with RNAi, the highest molecular mass band was absent from the protein blot (Fig. 2*A*). The same band is absent in *bpl-1* homozygotes, indicating that BPL-1 biotinylates the 242.6-kDa POD-2 isoform. We did not detect the lower molecular mass isoforms in our assay, which implies that the 242.6-kDa isoform is the most abundant biotinylated form under laboratory growth conditions.

The *pyc-1* gene encodes pyruvate carboxylase, which catalyzes the carboxylation of pyruvate to oxaloacetate in gluconeogenesis. The predicted molecular mass of PYC-1 is 129.3 and 67.8 kDa. Knockdown of *pyc-1* with RNAi resulted in reduction of intensity of the ~130 kDa protein band, and it is also reduced in *bpl-1* homozygotes.

BPL-1 is required for embryogenesis

Propionyl-CoA carboxylase converts propionyl-CoA to D-methylmalonyl-CoA in the breakdown of the branched-chain amino acids valine and isoleucine and in the metabolism of odd-chain fatty acids. Subsequent steps of D-malonylmalonyl-CoA metabolism provide succinyl-CoA to the tricarboxylic acid cycle. The presence of this pathway has been confirmed in *C. elegans* (11). The *C. elegans* genome contains orthologs for propionyl-CoA carboxylase subunits A and B (*pcca-1* and *pccb-1*). The *pcca-1* gene is predicted to encode a 79.7-kDa protein. Only PCCA-1 is predicted to contain a biotin-binding domain. Knockdown of *pcca-1* with RNAi caused a decrease in intensity of biotinylated protein bands at ~75 kDa (Fig. 2*A*). This protein

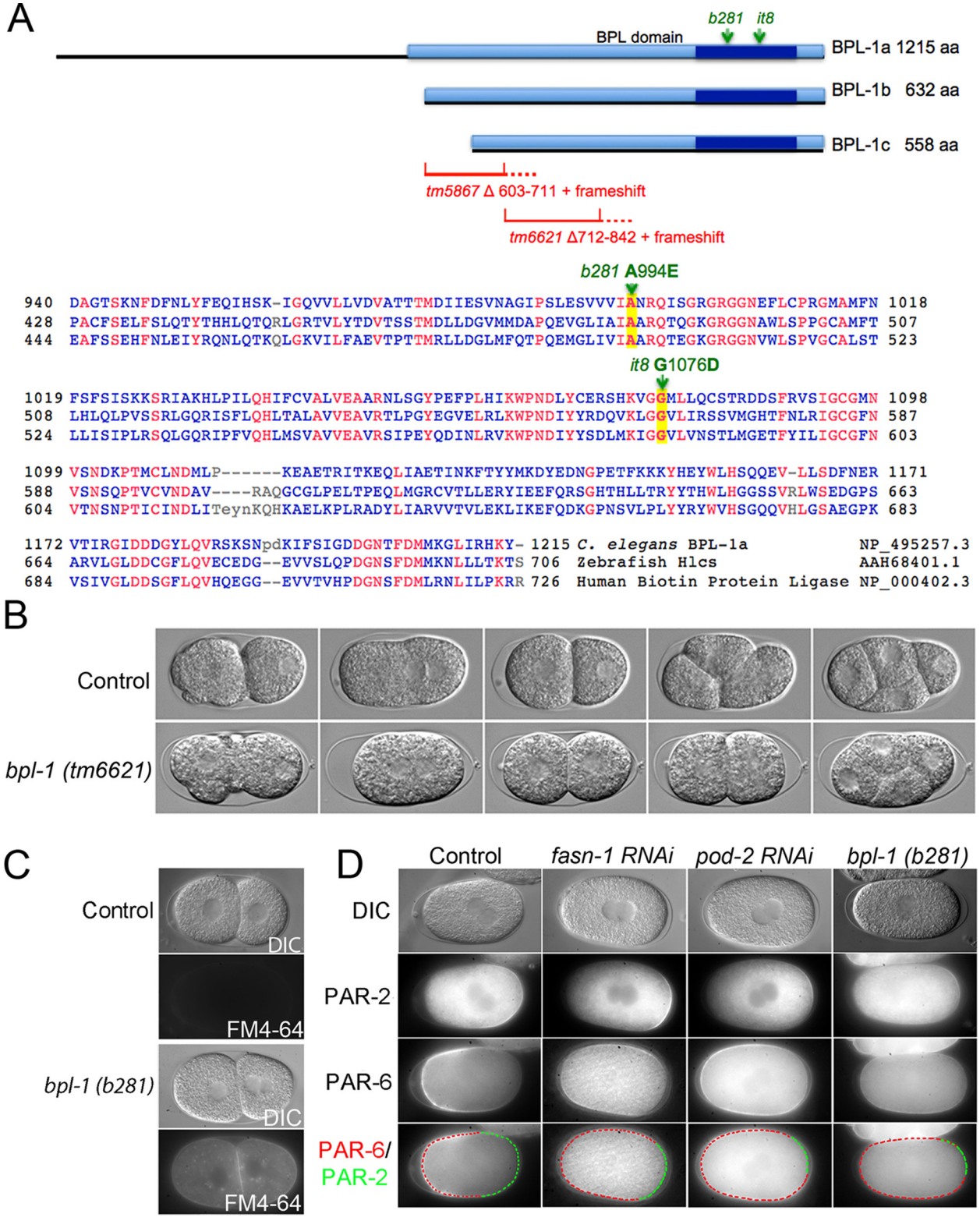

Table 1
Summary of *bpl-1*(*b281*) embryo phenotypes
Biotin was dissolved in water, and 5 μg was added to feeding plates. Oleic acid sodium salts were added to NGM at 0.1 mM with 0.1% Tergitol. Dye permeability was assayed with FM4-64. N, no rescue.

Phenotype	Control	*bpl-1 (b281)*	*bpl-1 (tm5867)*	*bpl-1 (tm6621)*
% Abnormal Spindle (N)	0% (20)	76% (17)	53% (17)	56% (18)
% Synchronous 2nd Division (N)	0% (20)	47% (17)	77% (17)	39% (18)
% Symmetric (N)	0% (20)	33% (21)	26% (23)	22% (18)
	bpl-1 (b281)	Biotin Rescue	Oleate Rescue	
Dye Permeability	100% (50)	N	N	
Constricted PAR-2 Domain	80% (15)	N	N	
2-Cell Multinucleation	87% (23)	N	N	
Dead Embryo	100% (976)	N	N	

band could contain a modified PCCA-1 protein, and it is reduced in *bpl-1* homozygotes.

The 3-methylcrotonyl-CoA carboxylase is also involved in branched-chain amino acid metabolism, converting 3-methylcrotonyl-CoA (derived from leucine) to 3-methylglutaconyl-CoA, which is further metabolized to acetyl-CoA and acetoacetate (1). Knockdown of *mccc-1* reduced intensity of the 73-kDa biotinylated protein band (Fig. 2*A*), indicating that *mccc-1* is the major biotinylated protein at 73 kDa.

To determine whether loss of carboxylase function explained the *bpl-1* embryonic phenotypes, we assessed viability and permeability of embryos when each of the carboxylases were knocked down by RNAi (Fig. 2, *B* and *C*). Mutations in the *pod-2* gene were previously shown to cause phenotypes very similar to those of *bpl-1* embryos (12, 13). We found that treating worms with RNAi against *pyc-1*, *pcca-1*, and *mccc-1* for 2 generations resulted in normal growth, impermeable embryos, and very low levels of embryonic lethality, similar to worms treated with an empty RNAi vector. Conversely, RNAi against *pod-2* starting at the L3 larval stage caused 100% permeable embryos and 100% embryonic lethality. Thus, these data provide evidence that loss of POD-2 biotinylation is responsible for embryonic defects caused by perturbed BPL-1 function.

Cytosolic, but not mitochondrial, fatty acid synthesis is required for C. elegans embryogenesis

Acetyl-CoA carboxylase, encoded by the *pod-2* gene in *C. elegans* (12), produces malonyl-CoA, which is a required substrate for several reactions, including cytosolic fatty acid synthesis, elongation of C16 and C18 fatty acids in the endoplasmic reticulum, and mitochondrial fatty acid synthesis. Interestingly, embryo phenotypes very similar to those we observe in *bpl-1* mutants have also been reported in a *pod-2* mutant and for RNAi knockdown of *fasn-1*, the major cytosolic fatty acid synthase gene of *C. elegans*. Early embryos of *pod-2(−) or fasn-1(RNAi)* exhibit egg shell permeability, multiple nuclei, cell cycle synchrony, and PAR protein mislocalization (Figs. 1*D* and 2*C*) (12).

In contrast, RNAi knockdown for genes required for mitochondrial fatty acid synthesis failed to show abnormal embryo phenotypes, although the disruption of mitochondrial synthesis of α-lipoic acid, which requires mitochondrial fatty acid synthesis, causes embryonic lethality in mice (14). Because malonyl-CoA is required for both cytosolic and mitochondrial fatty acid synthesis, we examined the embryo phenotypes of RNAi knockdowns for *mecr-1*, the mitochondrial *trans*-2-enoyl-CoA reductase (15). This RNAi knockdown did not result in embryo lethality or permeability, indicating that the fatty acid synthesis defects in *bpl-1* and *pod-2* mutants are probably mediated by the limitations of malonyl-CoA substrates required for cytosolic fatty acid synthesis and fatty acid elongation in the endoplasmic reticulum.

BPL-1 functions in fatty acid biosynthesis

To directly assess BPL-1's role in fatty acid synthesis, we used a stable isotope-labeling strategy that allows the identification of newly synthesized fatty acids as opposed to those obtained from the diet (16). We measured the relative proportion of newly synthesized fatty acids that animals accumulated over a 12-h period during the L4 larval stage and young adulthood. Knockdown of *bpl-1* led to reduced synthesis of several fatty acids, including the long-chain fatty acids 18:0, 18:1(*n*-7), and 18:2 by 25–50% (Fig. 3*A*), confirming that BPL-1 plays an important role in *de novo* fat synthesis. RNAi knockdown of *pod-2* also causes a reduction in *de novo* fat synthesis (17).

Knockdown of BPL-1 and other fat synthesis genes reduces embryonic polyunsaturated fats

We asked whether the reduction in fatty acid synthesis when *bpl-1*, *fasn-1*, or *pod-2* is knocked down causes changes to the overall proportions of fatty acids in the worm. Wild-type *C. elegans* contain a mix of saturated fatty acids, cyclopropane fatty acids, branched-chain fatty acids, and long-chain polyun-

Figure 1. Phenotypic analysis of *bpl-1* mutant embryos. *A*, mutations in the *C. elegans bpl-1* gene alter conserved biotin protein ligase residues. The *C. elegans bpl-1* gene encodes three protein isoforms (*black lines*) differing in length at the N terminus (WormBase WS251). These isoforms all contain the conserved biotin protein ligase/lipoyl protein ligase catalytic domain (BPL_LPL_catalytic domain IPR004143, amino acids 958–1141 in BPL-1a), indicated by a *dark blue bar* within a larger conserved biotin protein ligase domain (*lighter blue bar*, PTHR12835, amino acids 526–1215 in BPL-1a). The N-terminal region preceding the BPL domain of *C. elegans* BPL-1a is not conserved. The positions of the single amino acid changes produced by *b281* and *it8* mutations are within the conserved biotin-binding pocket of the protein and are indicated with *green arrows*. *tm5867* is a deletion resulting in removal of amino acids 603–711 and subsequent frameshift resulting in premature termination. *tm6621* is a deletion that removes codons for amino acids 712–842 and causes a frameshift and premature stop. Thus, neither deletion mutant retains the BPL domain. COBALT alignment between *C. elegans* BPL-1a and holocarboxylase synthetase proteins of human and zebrafish shows sequence conservation. Amino acid identities are in *red*. Amino acids changed by *C. elegans* point mutations are *highlighted* and indicated with *green arrows*. *b281* changes the codon for alanine 994 (*A*) to glutamic acid (*E*); *it8* changes the codon for glycine 1056 (*G*) to aspartic acid (*D*). Amino acid numbering is with respect to the longest BPL-1 isoform, BPL-1a. *B*, time-lapse differential interference contrast microscopy shows symmetric first cleavage in *bpl-1(tm6621)* and synchrony at the second division, compared with control embryos, which have asymmetric first cleavage and asynchronous second division. Both cells of the *bpl-1* two-cell embryo are shown divided transverse to the long axis of the embryo; in control embryos, only the posterior P1 cell divides with this orientation. Time-lapse movies from which these images were taken are included as Movie S1 (control) and Movie S2 (*bpl-1(tm6621)*). *C*, differential interference contrast (*DIC*) imaging of *bpl-1(b281)* two-cell embryo with multinucleation (*top*) and FM4-64 dye permeability (*bottom*). *D*, imaging of PAR-2:: GFP and PAR-6 ::mCherry in live embryos with compromised fatty acid synthesis. The PAR-2 domain is restricted, whereas the PAR-6 domain extends further into the posterior in *fasn-1* and *pod-2* RNAi and *bpl-1* mutant embryos than in controls. *Bottom*, outline of PAR-6 domain (*red*) and PAR-2 domain (*green*). The anterior is to the *left* and posterior is to the *right* in all images.

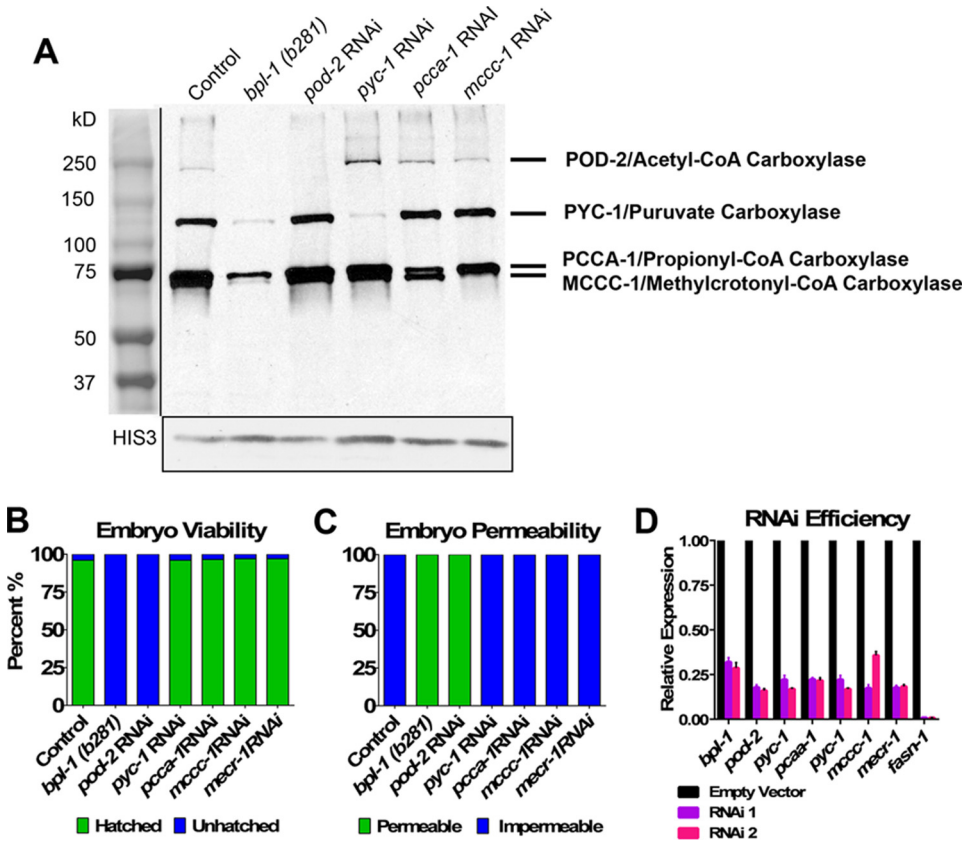

Figure 2. BPL-1 biotinylates carboxylase enzymes. *A*, Western blot probed with streptavidin to reveal biotinylated proteins. Total protein extracts from young adult *bpl-1(b281)* worms show reduced biotinylation compared with protein extracts from wild-type control. Also shown are biotinylated proteins in worms where each of the four carboxylase enzymes were knocked down with RNAi; in *bpl-1(b281)*, these carboxylase enzymes have reduced biotinylation. The same blot was probed with an antibody to histone 3 to serve as a loading control. *B*, percentage of hatched and unhatched embryos upon knockdown of genes encoding carboxylase enzymes and genes encoding mitochondrial fatty acid synthase II components by RNAi. Only knockdown of *pod-2* produced embryonic lethality similar to *bpl-1(b281)*. *C*, percentage of permeable and impermeable embryos upon knockdown of genes encoding carboxylase enzymes and genes encoding mitochondrial fatty acid synthase II components. Only knockdown of *pod-2* produced embryonic permeability defects similar to *bpl-1(b281)*. *D*, efficiency of RNAi knockdown. RNA was extracted from two biological replicates, RNAi 1 and RNAi 2, in young adult worms exposed to feeding RNAi constructs. Expression of the gene corresponding to the RNAi knockdown was determined by quantitative RT-PCR, using two reference genes as controls, shown relative to expression in the empty vector control. The RNAi knockdowns resulted in 3–100-fold reduction of transcript abundance. *Error bars*, S.E.

saturated fatty acids (PUFAs) (18). These fats are obtained both from the bacterial diet and by *de novo* synthesis (16). We used GC/MS to measure the fatty acid composition of late L4/young adult worms. Knockdown of *bpl-1* by RNAi slightly, but significantly, reduced the relative amounts of PUFAs and increased saturated fatty acids in worms (Fig. 3*B* and Table 2). Many of the fatty acids in *C. elegans*, including the 14- and 16-carbon saturated fatty acids, which are the end product of *de novo* synthesis, are obtained directly from the bacterial diet (19, 20), and these precursors can be elongated and desaturated to form a range of 18- and 20-carbon PUFAs (18). Our data demonstrate that nearly normal fatty acid composition of adult worms can be attained under conditions in which *de novo* fat synthesis is reduced.

Because *bpl-1* and *pod-2* depletion lead to maternal-effect lethality, we asked whether reduction of *de novo* fatty acid biosynthesis enzymes cause changes in embryonic lipids. We carried out parallel GC/MS analysis of embryos obtained by hypochlorite treatment of semi-synchronous, RNAi-treated *C. elegans*. Contrary to the subtle fatty acid changes in the whole worm lipid profile, knockdown of *bpl-1*, *pod-2*, or *fasn-1* resulted in drastic changes to the embryonic fatty acid composition: a >2-fold decrease in the total amount of PUFAs and an increased proportion of saturated fatty acids and cyclopropane fatty acids (Fig. 3*C* and Table 2). The dramatic decrease in embryonic PUFAs, which primarily are components of membrane phospholipids (21), suggests that membrane biophysical properties such as fluidity may be compromised.

Polyunsaturated fatty acids are required for early embryonic development

To test whether any of the embryonic defects observed in *bpl-1* were caused by loss of embryonic PUFAs, we examined mutants in the PUFA biosynthesis pathway. Synthesis of PUFAs requires the sequential addition of two double bonds to a saturated fatty acid by Δ9 and Δ12 desaturase enzymes (18). The *C. elegans* genome encodes three redundant Δ9 desaturases, FAT-5, FAT-6, and FAT-7 (22, 23), but only a single Δ12 desaturase, FAT-2. Mutations in the *fat-2* gene result in the accumulation of monounsaturated fatty acids and a nearly total loss of PUFAs (18), whereas the double mutant strain *fat-6;fat-7* has greatly increased saturated fatty acids and reduced PUFA composition, consisting of unusual PUFAs that are not normally synthesized (24).

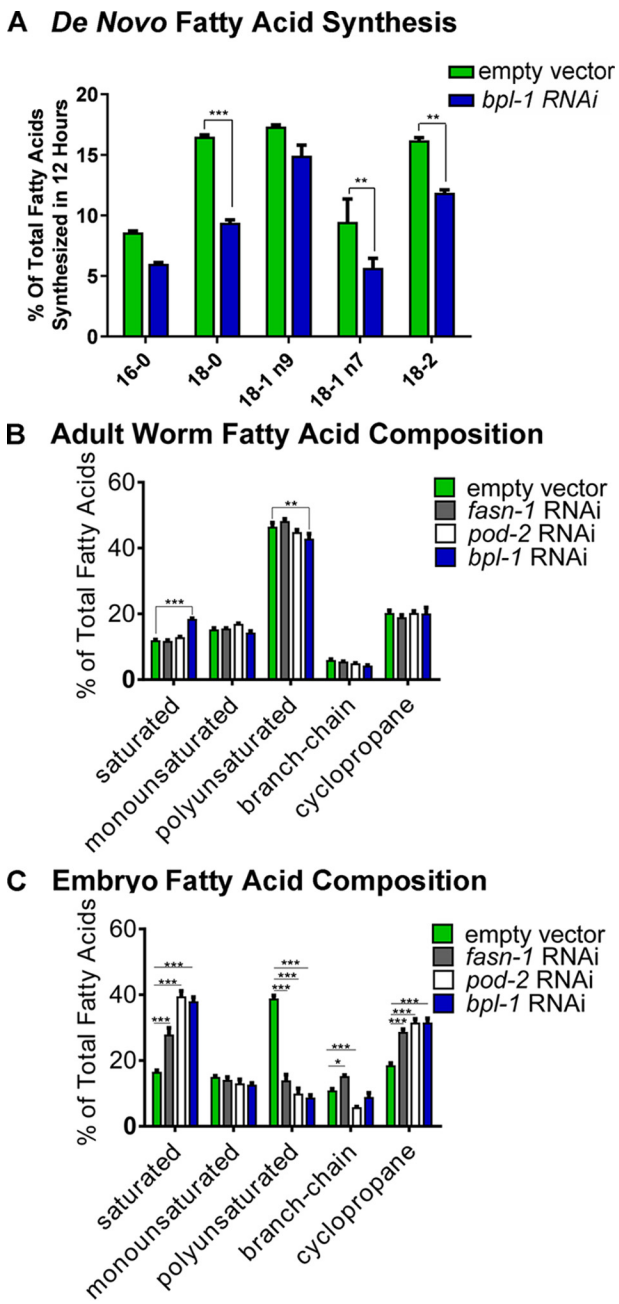

Figure 3. Loss of BPL-1 reduces *de novo* synthesis of fatty acids and alters embryonic fatty acid composition. *A*, the proportion of individual fatty acids produced by *de novo* synthesis was determined by labeling of the RNAi-hypersensitive *rrf-3*(*pk1426*) strain treated with RNAi feeding vectors or the empty vector control plasmid starting at the L4 larval stage. Labeling was achieved by feeding the worms a 1:1 (v/v) mixture of bacterial cultures that were grown in medium containing ^{13}C or in unlabeled medium containing ^{12}C. The percentage of *de novo* synthesized fatty acids was calculated after GC/MS analysis of isolated fatty acid methyl esters, where *de novo* synthesized isotopologs have masses corresponding to carbon chains consisting of a mixture of ^{12}C and ^{13}C carbons, whereas dietary fatty acids that are incorporated intact contain 100% ^{12}C or ^{13}C fatty acids. *Bars*, mean and S.E. (*error bars*). Knockdown of *bpl-1* reduced *de novo* synthesis of 16- and 18-carbon fatty acids. *B*, relative fatty acid composition of young adult worms grown on *fasn-1*, *pod-2*, or *bpl-1* RNAi bacteria compared with L4440 (empty vector) controls. *C*, fatty acid composition of embryos isolated from adult worms by hypochlorite treatment. Relative values of individual fatty acids are reported in Table 2. Saturated fatty acids include 14:0, 16:0, and 18:0; polyunsaturated fatty acids include 18:2, 18:3, 20:3, 20:4, 20:4(*n*-3), and 20:5; branched-chain fatty acids include 15:iso and 17:iso; and cyclopropane fatty acids include 17Δ and 19Δ. *Bars*, means with S.E. (*error bars*). *, $p < 0.05$; **, $p < 0.005$; ***, $p < 0.0005$.

We found that similar to *bpl-1* mutants, mutations in *fat-2* and, to a lesser extent, *fat-6;fat-7* resulted in embryonic lethality, disruption of the permeability barrier, and aneuploidy (Fig. 4, *A* and *B*). The penetrance of these embryonic abnormalities was incomplete, suggesting that disruption of PUFA synthesis cannot entirely explain the embryonic defects caused by mutations in the genes encoding earlier components of the fat biosynthesis pathway. However, these genetic data provide strong evidence that PUFAS are important for the formation of the embryonic permeability barrier and that the embryonic defects resulting from loss of BPL-1, POD-2, and FASN-1 are at least partially due to reduction of PUFAs.

To further investigate the role of PUFAs in the early embryo, we supplemented the *C. elegans* diet with either the monounsaturated fatty acid, oleic acid, or with the PUFA, linoleic acid, and assessed lethality and permeability in embryos of fat-supplemented animals compared with controls. Treatment with the 18-carbon PUFA linoleic acid, but not the monounsaturated fatty acid oleic acid, rescued embryonic lethality and permeability barrier defects in *fat-2,* confirming that PUFAs, but not MUFAs, are critical for the early embryo (Fig. 4, *C* and *D*). Interestingly, neither supplemental MUFAs nor PUFAs rescued embryonic lethality or permeability barrier defects in *bpl-1(it8)*. That *bpl-1* is not rescued by supplemental PUFAs probably means that simpler fatty acid precursors, such as malonyl-CoA, are needed for *de novo* synthesis of complex permeability barrier components. Given the requirement for cytochrome P450s, cytochrome P450 reductase, and the putative sugar-modifying enzyme PERM-1 for the formation of the permeability barrier (25, 26), malonyl-CoA synthesis could be required for *de novo* synthesis and/or elongation of PUFAs as well as for synthesis of a complex lipid, such as a hydroxylated glycosphingolipid. Because these types of complex lipids are digested by lipases upon ingestion by *C. elegans*, it is not possible to test these molecules for rescue by dietary supplementation.

Bacterial sources of malonyl-CoA or other fatty acid precursors compensate for BPL-1 activity during larval growth and development but not during embryogenesis

Previous studies showed that both ACC/POD-2 and FASN-1 are needed for synthesis of specific sphingolipids during larval development. Knockdown of either gene caused defects in the intestinal lumen and early embryonic arrest due to a defect in the synthesis of glucosylceramides (27, 28). Thus, the ability of homozygous *bpl-1* deletion mutant strains to develop normally throughout their larval growth stages was puzzling, because malonyl-CoA is required for fatty acid synthesis reactions catalyzed by ACC/POD-2 and FASN-1.

The finding that *bpl-1* depletion only modestly reduced *de novo* lipid synthesis in young adult nematodes (Fig. 3*A*) led us to hypothesize that *C. elegans* obtains precursors for *de novo* fatty acid synthesis, such as malonyl-CoA, malonate, or short-chain fatty acids, directly from their bacterial diet to support lipid biosynthesis. Malonyl-CoA levels are highly regulated in animal cells; however, malonyl-CoA has been shown to be present in micromolar concentrations in the intracellular pool of *Escherichia coli* (29). To test whether bacterial fatty acid precursors

Table 2

Fatty acid composition of adult worms and embryos

Fatty acid nomenclature is as follows: *x*:*y*(*n*-*z*), where *x* represents the number of carbons, *y* is the number of double bonds, and *n*-*z* is the location of terminal double bonds, *z* carbons from the methyl end. 15:iso, 13-methyltetradecanoic acid; 17:iso, 15-methylhexanoic acid; 17Δ, *cis*-9,10-methylenehexadecanoic acid; 19Δ, *cis*-11,12-methylene octadecanoic acid. *, $p < 0.05$; **, $p < 0.005$; ***, $p < 0.0005$.

	14:0	15iso	16:0	17iso	16:1	17Δ	18:0	18:1n-9	18:1n-7	18:2n-6	19Δ	18:3:n-6	20:3n-6	20:4n-6	20:4n-3	20:5n-3
Adult Worms																
1-Way ANOVA	P=0.0002	P=0.84	P<0.0001	P<0.0001	P=0.01	P=0.89	P=0.35	P=0.002	P=0.17	P=0.0091	P=0.27	P=0.0015	P=0.02	P=0.26	P=0.02	P=0.74
empty vector	**1.34**	**2.87**	**3.75**	**3.10**	**1.63**	**14.71**	**6.89**	**2.83**	**10.80**	**6.16**	**5.57**	**1.90**	**5.46**	**2.18**	**6.65**	**24.18**
empty vector (SD)	0.21	0.68	0.24	0.33	0.44	2.55	0.72	0.19	0.97	0.48	0.58	0.15	0.31	0.13	0.70	2.79
fasn-1(RNAi)	**1.52**	**2.66**	**3.91**	**2.85**	**1.80**	**14.23**	**6.34**	**2.58**	**11.17**	**5.51**	**4.74**	**2.17**	**5.31**	**2.21**	**6.88**	**26.12**
fasn-1 (SD)	0.16	0.30	0.28	0.13	0.25	2.16	0.63	0.13	0.41	0.39	0.39	0.23	0.85	0.14	0.42	1.67
P-Value																
pod-2(RNAi)	**1.93**	**2.52**	**5.14**	**2.47**	**2.81**	**15.73**	**5.86**	**2.19**	**11.96**	**5.16**	**4.53**	**2.20**	**4.59**	**1.95**	**6.34**	**24.62**
pod-2(SD)	0.32	0.23	0.23	0.12	0.35	1.78	0.62	0.14	0.60	0.17	0.49	0.13	0.36	0.10	0.34	1.68
P-Value			**	*	*			*								
bpl-1(RNAi)	**3.19**	**2.78**	**8.96**	**1.49**	**2.52**	**15.94**	**6.30**	**1.73**	**10.07**	**4.43**	**4.16**	**3.52**	**3.86**	**1.95**	**5.35**	**23.75**
bpl-1(SD)	0.42	0.64	0.45	0.18	0.42	4.93	0.64	0.38	1.38	0.62	1.40	0.60	0.30	0.32	0.43	4.08
P-Value	***		***	***	*			**		**		**	*		*	
Embryos																
1-Way ANOVA	P=0.0002	P=0.14	P<0.0001	P<0.0001	P=0.09	P=0.0003	P=0.13	P<0.0001	P=0.63	P=0.0002	P=0.03	P=0.05	P=0.01	P=0.13	P<0.0001	P<0.0001
empty vector	**1.93**	**5.59**	**6.36**	**5.34**	**1.66**	**13.06**	**8.31**	**3.10**	**10.29**	**6.62**	**5.50**	**1.22**	**3.32**	**1.57**	**5.88**	**20.25**
empty vector (SD)	0.54	1.35	0.58	0.16	0.42	1.68	1.69	0.34	1.00	0.50	0.63	0.26	0.40	0.27	0.73	1.98
fasn-1(RNAi)	**2.88**	**7.65**	**10.85**	**7.61**	**1.62**	**19.57**	**14.18**	**2.68**	**9.81**	**4.23**	**9.17**	**0.52**	**1.98**	**0.77**	**1.81**	**4.67**
fasn-1 (SD)	0.38	0.66	2.08	1.25	0.56	1.69	4.50	0.33	1.95	1.18	1.64	0.40	1.02	1.05	0.91	1.84
P-Value				*		*				*	*				***	***
pod-2(RNAi)	**6.05**	**3.84**	**25.57**	**2.00**	**3.10**	**25.31**	**7.91**	**1.21**	**8.78**	**2.28**	**6.26**	**1.27**	**1.09**	**0.42**	**1.09**	**3.83**
pod-2(SD)	0.59	0.30	3.08	0.35	1.09	2.42	2.51	0.18	2.59	0.67	0.98	0.48	0.75	0.50	0.73	1.80
P-Value	***		***	**		***		***		***			*		***	***
bpl-1(RNAi)	**5.66**	**6.63**	**23.02**	**2.31**	**2.77**	**24.95**	**9.36**	**1.23**	**8.68**	**2.29**	**6.63**	**2.12**	**0.73**	**0.32**	**0.72**	**2.56**
bpl-1(SD)	1.03	3.25	1.76	0.62	0.71	2.57	3.06	0.14	0.93	0.20	1.35	0.88	0.61	0.33	0.32	0.67
P-Value	***		***	**		***		***		***			**		***	***

were providing sufficient metabolites for lipid synthesis during larval development, we provided a malonyl-CoA–restricted food source by feeding K12-derived *E. coli* L8, containing a temperature-sensitive mutation in the *accB* gene, which encodes the β-subunit of the *E. coli* acetyl-CoA carboxylase. Growth of the bacteria at restrictive temperature depletes malonyl-CoA stores and impedes new bacterial lipid synthesis compared with L8 grown at non-restrictive temperature.

Growth and lipid composition of both wild-type and *bpl-1* mutant *C. elegans* larvae fed L8 bacteria grown at non-restrictive temperature were comparable with those of *C. elegans* grown on the *E. coli* strain OP50. In contrast, we found that *bpl-1(b281)* mutants were much more severely affected than wild type when fed acetyl-CoA carboxylase–restricted L8 bacteria that were grown at restrictive temperature; *bpl-1(b281)* worms arrested growth at the L3 larval stage, whereas wild-type worms reached adulthood but had a smaller size. A small proportion of wild type arrested similarly to *bpl-1* (Fig. 5, *A*–*C*). Growth of both *bpl-1* and wild type was completely rescued by supplementation with biotin (Fig. 5, *A* and *B*), but not oleate, malonate, or malonyl-CoA (not shown). This is in contrast to the embryonic phenotypes described above, where neither biotin nor supplemented fatty acid precursors or fatty acids are able to rescue the permeability barrier and polarity defects of embryos produced by *bpl-1* mutant mothers.

Finally, we tested the ability of worms to synthesize fatty acids when dietary malonyl-CoA and other fatty acid precursors were restricted. Interestingly, wild-type worms significantly increased *de novo* fat synthesis in response to the L8 diet (Fig. 5*D*), suggesting that the worms can detect dietary malonate and other fatty acid precursors and increase *de novo* synthesis to compensate when these dietary substrates are limited. Together, these data indicate that *C. elegans* maintains a balance of malonate or other precursors obtained from the diet and malonyl-CoA synthesized *de novo* from acetyl-CoA to support lipid synthesis for larval growth and development but that dietary lipids and precursors are not available or are not utilized during oogenesis and embryogenesis, and thus *de novo* synthesized lipids are required at this stage (Fig. 5, *E* and *F*).

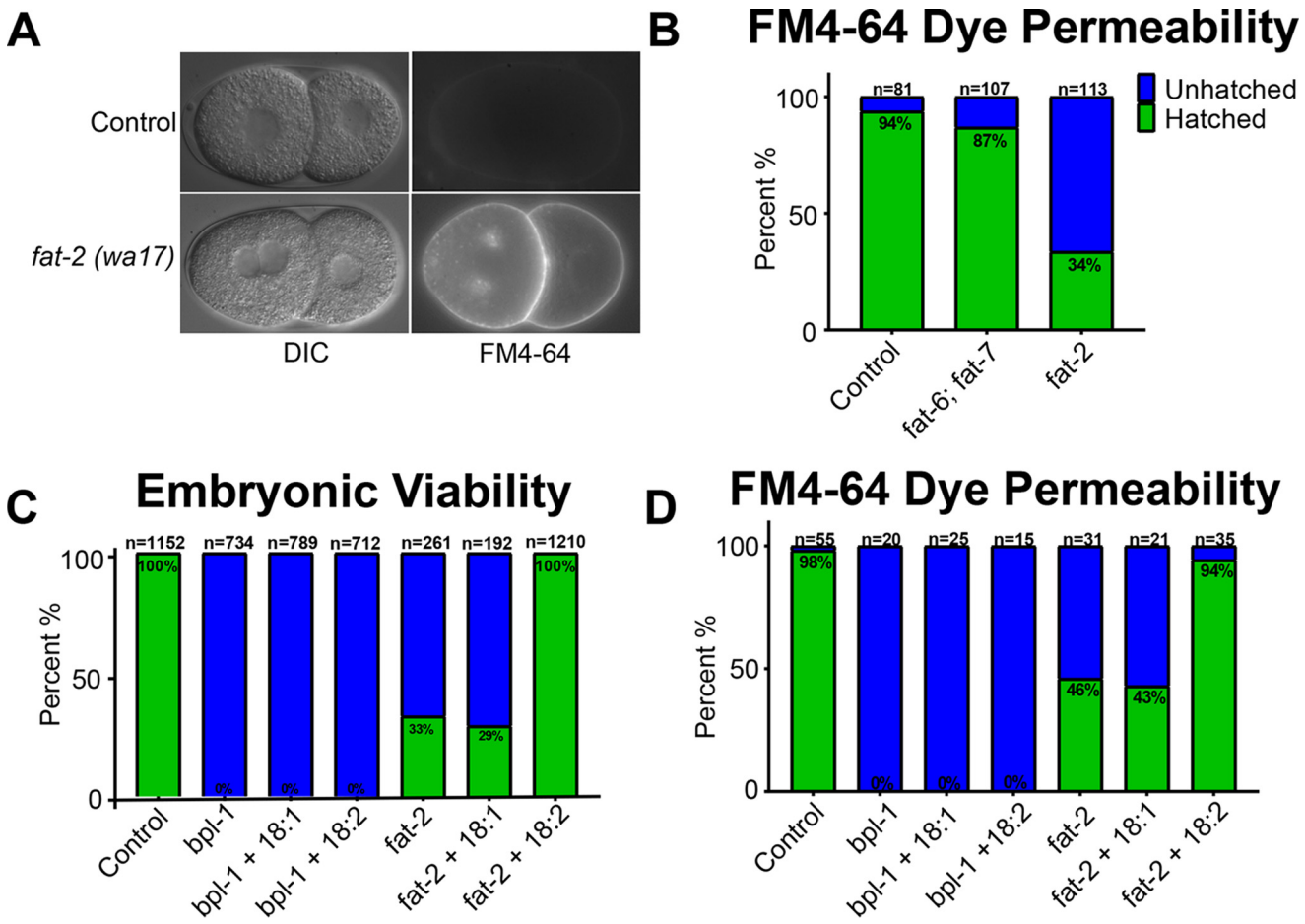

Figure 4. Polyunsaturated fatty acids are required for meiosis and synthesis of the embryonic permeability barrier. *A*, representative image of *fat-2(wa17)* loss of function mutant, compared with wild type (control), showing multiple nuclei in the anterior blastomere at the two-cell stage. *B*, quantification of FM4-64 dye permeability in fatty acid desaturase mutants *fat-6;fat-7* and *fat-2*. *C* and *D*, treatment of wild-type (control), *bpl-1(it8)*, or *fat-2(wa17)* mutant worms with 0.1 mM oleic acid (18:1), linoleic acid (18:2), or carrier 0.1% Tergitol. Treatment with 18:2 rescues embryonic lethality (*C*) and FM4-64 dye permeability (*D*) in *fat-2* but not *bpl-1*. *Error bars*, S.E.

Discussion

We have demonstrated that the *C. elegans* gene *bpl-1* encodes a biotin-ligating enzyme homologous to mammalian holocarboxylase synthetase. BPL-1 is required for normal biotinylation of at least four conserved carboxylase enzymes. Mutations in the conserved biotin-binding domain of BPL-1 are detrimental to embryonic and larval development. Further, by knocking down each of four carboxylase genes with RNAi, we showed that reduction of the POD-2 acetyl-CoA carboxylase produces embryonic defects similar to *bpl-1* mutants, whereas reduction of other carboxylase gene products showed no detrimental developmental effects. Thus, under laboratory conditions when nutrients are abundantly available, *de novo* fatty acid synthesis and fatty acid elongation, reactions that required malonyl-CoA produced by acetyl-CoA carboxylase, are the primary biotin-dependent pathways affected by loss of BPL-1.

BPL-1 plays a central role in lipid *de novo* fatty acid synthesis and elongation and is required for the synthesis of the embryonic permeability barrier and polarity in the embryo. Embryo production is a major consumer of nutrients, and young adult hermaphrodites convert their body mass to embryos every 24 h (30). Bacterial nutrients provide intact fatty acids as well as precursors, such as malonyl-CoA, for growth and development. Our finding that loss of *de novo* synthesis genes causes a large reduction of PUFAs in embryos, but not in the adult worm, supports a model in which dietary fatty acid precursors and *de novo* synthesized malonyl-CoA and fatty acids contribute to the lipid requirements for rapid growth and development during larval stages. However, in the sequestered environment of the early embryo, dietary support is unavailable and lipid incorporation is dependent on *de novo* synthesis and elongation, particularly for PUFA production. Stable isotope labeling studies indicate that PUFAs are preferentially synthesized from *de novo* derived, as opposed to dietary, precursors (16, 17). The inaccessibility of dietary fats during the oocyte– embryo transition perhaps ensures that fresher, less oxidized fatty acids are present at the start of embryonic life. In addition to providing precursors for membrane and storage lipid synthesis, recent studies revealed that fatty acid levels signal environmental conditions that influence sex determination in nematodes (31), and microbial metabolites, including lipid precursors, affect host metabolism, influencing reproduction and lifespan (32–34).

The embryonic permeability barrier performs the critical function of maintaining osmotic integrity of the embryo. Depletions of the lipid biosynthetic genes *pod-2* and *fasn-1* both

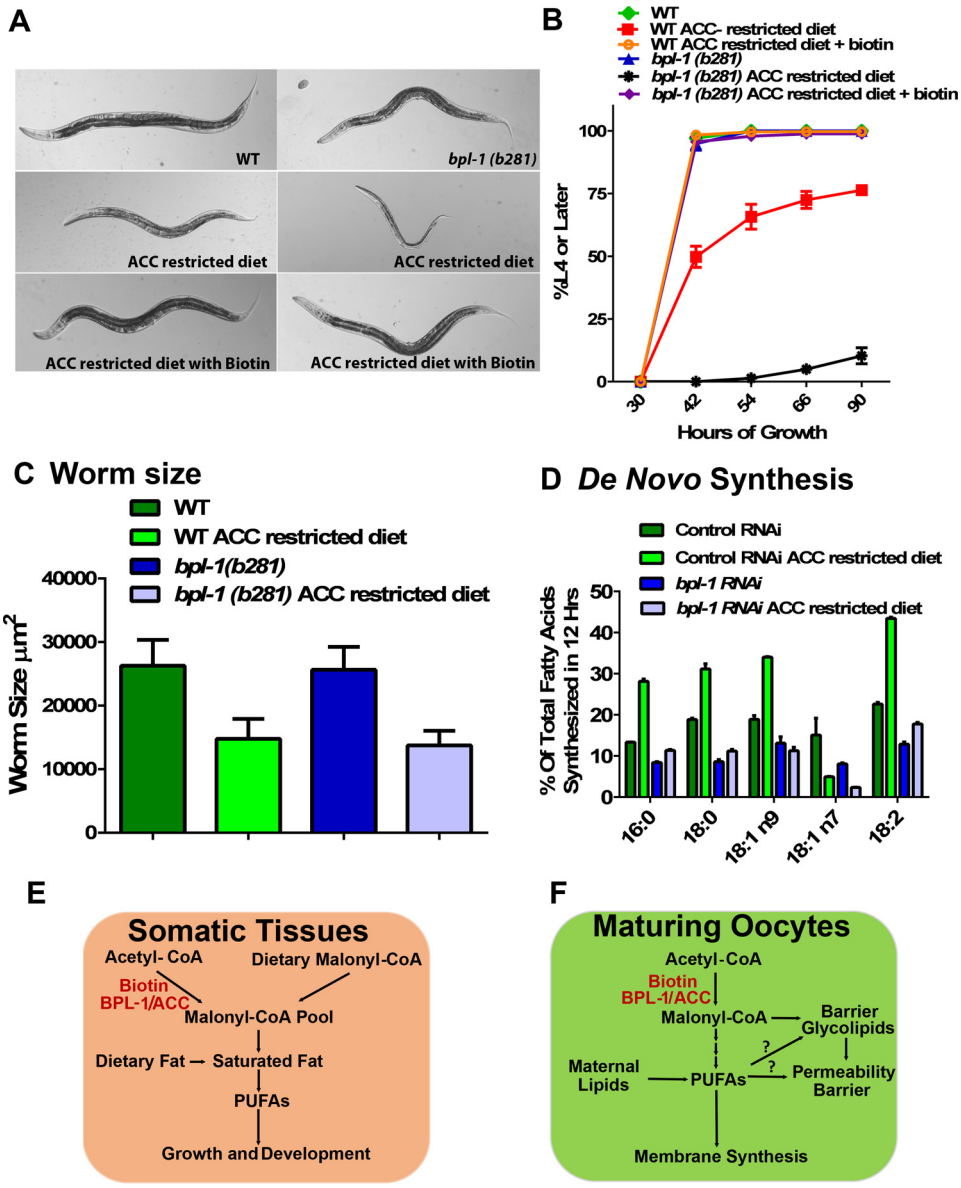

Figure 5. Dietary fatty acid precursors support larval growth in the absence of BPL-1. *A*, images show WT or *bpl-1(b281)* adults grown on either non-restricted *E. coli* (L8 grown at permissive temperature) or ACC-restricted bacteria (L8 grown at restrictive temperature) for 66 h. Larval development is arrested in *bpl-1(b281)* when bacterial fatty acid precursors are restricted. However, growth is rescued by the addition of 5 μg of biotin to feeding plates. *B*, a diet of L8 bacteria grown at restrictive temperature causes arrested development in *bpl-1(b281)* and, to a lesser extent, in wild type. *C*, a diet of L8 bacteria grown at restrictive temperature reduces body size of wild-type and *bpl-1(b281)* worms at 42 h of growth. *D*, *de novo* synthesis of individual fatty acids is increased in wild type when fatty acid precursors are restricted from the diet, but not in *bpl-1(b281)*. The RNAi-hypersensitive *rrf-3*(*pk1426*) strain was treated with RNAi or the empty vector control plasmid starting at the L4 larval stage. Their progeny were fed at L4 larval stage for 12 h on HT115 bacteria grown in medium containing a mix of ^{12}C and ^{13}C media (1:1, v/v). *E* and *F*, model depicting dietary *versus* synthetic sources of malonyl-CoA during somatic development and during the oocyte–embryo transition.

cause osmotic integrity defects, as does loss of EMB-8, the NADPH reductase, and two lipid-modifying cytochrome P450 enzymes, as well as the putative sugar-modifying enzyme PERM-1 (12, 25, 26), which suggests that the permeability barrier may contain glycosylated and hydroxylated lipids. We have demonstrated that permeability barrier defects caused by depletion of lipid biosynthesis genes result, at least partially, from loss of embryonic PUFAs, which could be incorporated into the barrier as a component of complex hydroxylated glycolipids. In mammals, the PUFAs linoleic and linolenic acid are required for the synthesis of the impermeable corneocyte lipid envelope of the skin, in which PUFAs are esterified to the ω-hydroxyl of the amide-linked very-long-chain fatty acid of a unique class of esterified ceramides (35). A cytochrome P450 enzyme is required for the ω-hydroxylation, and lipoxygenase enzymes are proposed to further oxidize the esterified ceramides to allow binding of the lipid to proteins of the cell envelope, forming the permeability barrier (35, 36).

Similar to other permeability barrier genes, *bpl-1* is important for embryonic polarity. We found that loss of *bpl-1* caused symmetric first divisions, restricted PAR-2 domains, synchronous second divisions, and transverse spindle orientations during the second division. The relationship between the permeability barrier and polarity is not understood. The permeability

barrier could affect polarity via direct interactions between the barrier and the cell membrane or cell cortex, or polarity defects could result from loss of osmotic regulation. Alternatively, the polarity defects associated with fat synthesis could be independent of permeability barrier function. Previous work suggested that *pod-2*– and *emb-8*– depleted embryos displayed weakened interaction between the paternal pronucleus and the cell cortex, which correlated with symmetric first divisions (12). This weakened interaction with the cortex could be explained by either a defective interaction with the permeability barrier or altered embryonic membrane composition. Future work is needed to determine the structure and function of the specific lipids that compose the permeability barrier and how they influence polarity.

The rate-limiting step in *de novo* fatty acid synthesis is carboxylation of acetyl-CoA by acetyl-CoA carboxylase to generate malonyl-CoA. In humans, holocarboxylase synthetase deficiency is an autosomal recessive disorder that usually manifests early in life, with patients showing defects in fatty acid biosynthesis, gluconeogenesis, and amino acid metabolism that lead to severe conditions of the skin, damage to the nervous system, coma, and early death (37). Fortunately, continual supplementation with biotin is sufficient to treat the syndrome in most cases, suggesting that excess biotin can drive carboxylase reactions in the absence of fully functioning holocarboxylase synthetase (5). Due to rapid turnover, it is not generally believed that appreciable malonyl-CoA pools accumulate during fatty acid synthesis (38, 39). Despite this, our work demonstrates that *C. elegans* uses both dietary fatty acid precursors and *de novo* synthesized malonyl-CoA for lipid synthesis. Restricting dietary fatty acid precursors by feeding *E. coli* deficient in acetyl-CoA carboxylase activity caused severe arrest during larval development in worms without functioning BPL-1 and even showed a measurable effect on growth in wild-type worms. Dietary biotin rescues these growth deficiencies in both wild type and the *bpl-1* mutants.

Our studies indicate that *C. elegans* obtain malonyl-CoA from both dietary precursors and from acetyl-CoA carboxylase reactions. Our observation that supplemental biotin rescued larval development is consistent with the success of treatments for holocarboxylase synthetase deficiency in humans, although it is not known whether holocarboxylase synthetase– deficient humans treated with dietary biotin experience fertility loss or birth defects in their offspring. Furthermore, malonyl-CoA is an important regulator of lipid metabolism. In hepatocytes, malonyl-CoA levels regulate the balance between fat synthesis and fatty acid oxidation (40, 41). We found that in *C. elegans*, loss of dietary fatty acid precursors caused an increase in *de novo* fatty acid synthesis, demonstrating that *de novo* fat synthesis is regulated depending on the availability of dietary precursors.

This study is the first to characterize the *C. elegans* holocarboxylase synthetase, BPL-1. Holocarboxylase synthetase is a critical regulator of biotin utilization at the epicenter of multiple metabolic pathways. Here, we demonstrated that BPL-1 function is critical for maintaining fatty acid composition during embryonic development, establishment of embryonic polarity, integrity of the embryo permeability barrier, and support of post-embryonic development. In addition to the role of HCS in metabolism, the enzyme also appears to play a role in gene regulation through biotinylation and direct interaction with histones (42–44). Study of HCS function in *C. elegans* will provide a powerful tool for dissecting the diverse roles of HCS in a multicellular organism under different environmental and dietary conditions.

Experimental procedures

C. elegans strains and RNAi

Nematodes were maintained on nematode growth medium (NGM) at 20 °C seeded with *E. coli* (OP50) unless otherwise stated (45). The wild-type strain was N2, and the *mel-3(b281)* and *mel-3(it8)* mutants were isolated in screens for maternal-effect lethal mutations (7) and maintained as heterozygotes over the *mnC1* balancer as *mel-3(b281 or it8) unc-4(e120)/mnC1 II*. Strains carrying deletions for deletion mapping with *mel-3* mutants were provided by the *Caenorhabditis* Genetics Center. Two deletion alleles, *tm5867* and *tm6621*, were obtained from the Mitani laboratory, Tokyo Women's Medical University School of Medicine. These were outcrossed, marked with *unc-4(e120)*, and balanced with *mnC1*. Deletion end points of *tm5867* and *tm6621* were confirmed by DNA sequence analysis.

Transformation rescue of *b281* and *it8* mutants with cosmid or plasmid DNA was performed as described (46). Approximately 6.5 kb of the *bpl-1* gene, including 600 bp upstream of the first predicted transcription start point, were sequenced from *b281* and *it8* homozygous worms. Only a single point mutation was found for each mutant.

Feeding RNAi experiments used NGM supplemented with 100 μg/ml ampicillin, 2 mM isopropyl β-D-1-thiogalactopyranoside and seeded with the appropriate HT115 RNAi bacteria. Feeding RNAi was performed by plating embryos of the RNAi-sensitive strain *rrf-3*(*pk1426*) onto seeded RNAi plates, with the exception of RNAi of *pod-2* and *fasn-1*, in which feeding RNAi was initiated at the L3 larval stage. The *pod*-2, *fasn-1*, *mecr-1*, and *pyc-1* feeding constructs were obtained from the Ahringer RNAi library and verified by sequencing (47) (Source BioSource). For RNAi of *bpl-1*, *pcca-1*, and *mccc-1*, a 250–550-bp portion of each gene was amplified from N2 DNA using primer sequences TTCTTCGATTTGCATTTGGGAGTC and GTTTCCGGGCCATTATCCTCAT for *bpl-1*, GGTAGTGTGGGGGCCAGGAT and TTTTGAAGGGCAGCCAAAGC for *mccc-1*, and CTTGAGAAGGCTGGAGCCAA and CGAGGAATTCGACGGTT for *pcca-1*. Amplified DNA was cloned into L4440, and RNAi constructs were sequence-verified. Empty vector L4440 was used as the control.

RNA extraction and quantitative RT-PCR

RNA was extracted from ~2000 nematodes using 1 ml of TRIzol reagent and multiple freeze–thaw cycles to break up nematodes. After chloroform addition and phase separation, the aqueous phase was precipitated with isopropyl alcohol, and RNA was further purified using a Qiagen RNeasy Plus minikit with genomic DNA eliminator column as per the manufacturer's instructions. cDNA was synthesized from 1 μg of RNA using oligo(dT) primer and superscript IV. Real-time quantita-

tive PCR was performed in triplicate on each of two biological replicates using PowerUp SYBR Green master mix (Applied Biosystems) using an Applied Biosystems 7300 real-time PCR system. The $\Delta\Delta Ct$ method was used to determine the relative expression of the target gene in the RNAi knockdowns compared with empty vector controls. The ΔCt values were calculated using the geometric mean of the *Ct* values for two reference genes, *tbb-2* and *Y45F10D.4* (Fig. 2*D*).

Microscopy

To image live embryos, adult worms were dissected with a syringe needle in 0.8× egg buffer on a glass coverslip and compressed against a pad of 1% agarose dissolved in 0.8× egg buffer and cushioned with petroleum jelly (48). To visualize eggshell defects, 2–6 μM FM4-64 (Thermo Fisher catalog no. T-3166) dye was added to the dissecting buffer (26). Imaging was performed on a Leica DM RA2 microscope with Hamamatsu Orca-ER using OpenLab (Improvision) or BioVision software. Additional imaging was performed on an Olympus BX53 microscope with a QImaging Retiga 2000R CCD camera and analyzed with the QCapture software and ImageJ. Embryo permeability was confirmed for all *bpl-1* alleles using Nile Blue A uptake (49).

PAR-2 and PAR-6 localization in living early embryos was visualized with the transgenes *itIs272*[*Ppar-6:: par-6::mCherry*] (50), and *itIs297*[*Ppie-1:: par-2::gfp + unc-119(+)*] (provided by Aaron Schetter). The *unc-4*–marked *bpl-1* mutants *b281*, *tm5867*, and *tm6621* were each crossed into KK1213 *itIs272*[*Ppar-6:: par-6::mCherry + unc-119(+)*]; *itIs297*[*Ppie-1:: par-2::gfp + unc-119(+)*] to create the strains KK1205, KK1212, and KK1230, respectively. To confirm PAR protein mislocalization phenotypes in *b281*, *it8*, *tm5867*, and *tm6621* without transgenes, we fixed *unc-4 bpl-1* and control *unc-4* worms and embryos on slides in methanol at −20 °C and stained with primary antibodies to PAR-2 (51) and PAR-3 (52). AF488– or Cy-3–labeled secondary antibodies were from Invitrogen and Jackson ImmunoResearch.

Meiosis was examined in *bpl-1* oocytes and fertilized zygotes *in utero* using strain KK1193 *bpl-1(b281) unc-4(e120)/mnC1 II; unc-119(ed3) ruIs32*[*Ppie-1:: gfp::H2B + unc-119(+)*] *III* and their heterozygous siblings from the same strain, which have fully viable embryos. *ruIs32* was derived from strain AZ212 (53).

Protein blot detection of biotinylated proteins

To extract worm protein, 300 young adult worms were collected in M9 buffer and allowed to settle on ice before washing one time with M9, resettling on ice, and then removing the supernatant until ~20 μl of worm pellet remained. We then added 20 μl of 2× Laemmli buffer and boiled the samples for 5 min. After boiling, each sample was Dounce-homogenized 100× with the melted end of a pipette tip and frozen at −20 °C. Before use, samples were reheated to 90 °C.

Proteins were separated by SDS-PAGE with Bio-Rad 7% Mini-Protean precast gels and transferred with Towbin buffer with no SDS for 20 min using semidry transfer onto PVDF membranes. Membranes were blocked with 2% BSA in PBST (0.05% Tween 20). We probed for biotinylated proteins by incubating the membranes with 2 μl of streptavidin-horseradish peroxidase conjugate (Abcam ab7403; 1 mg/ml) in 10 ml of PBST (0.1% Tween 20) for 30 min, followed by washing with PBST (six 7-min washes). Bands were visualized using the Pierce ECL Western blotting substrate with a 2-min incubation time. Biotinylated proteins were visualized on X-ray film, and protein standards (Bio-Rad dual color standards) were visualized using a Bio-Rad imager.

Lipid extraction for fatty acid composition

Lipids were extracted as described previously (21). Briefly, worms were washed from feeding plates with water, washed once to remove residual bacteria, and allowed to settle on ice. After residual water was removed, the worm pellet was incubated for 1 h at 70 °C in 2.5% sulfuric acid in methanol. After stopping the reaction with water, the fatty acid methyl esters were extracted with hexane.

Stable isotope labeling assay

As described elsewhere (16, 17), to quantify the amount of *de novo* fatty acid synthesis, worms were fed a mixed culture of *E. coli*, where bacteria was grown in either LB broth or ^{13}C-labeled Isogro medium (Sigma-Aldrich). Overnight cultures of each were pelleted and mixed (1:1, v/v) after resuspension to 0.075 mg/ml in M9. The RNAi-hypersensitive *rrf-3*(*pk1426*) strain was treated with RNAi or the empty vector control plasmid starting at the L4 larval stage. Their progeny were fed for 12 h starting at the L4 larval stage on HT115 bacteria grown in medium containing a mix of ^{12}C and ^{13}C media (1:1, v/v).

Lipid analysis

Fatty acid methyl esters were analyzed by GC/MS using an Agilent 7890 GC/5975C MS. For *de novo* synthesis experiments, we operated the MS in scanning mode to monitor ions *m*/*z* 260–300 for 16 carbon fatty acids and *m*/*z* 290–320 for 18 carbon fatty acids. The percentages of individual fatty acids that derived completely via *de novo* synthesis from acetyl-CoA were determined using the ratio of ions *m*/*z* 273–283 to total isotopologs for 16 carbon fatty acids and the ratio of ions *m*/*z* 290–314 for 18 carbon fatty acids.

Isolation of embryos for lipid analysis

To isolate early embryos for lipid analysis, worms were synchronized with hypochlorite treatment, and isolated eggs were allowed to hatch and develop on *bpl-1* RNAi plates until adult stage. Embryos were collected from the uteri of adult worms by hypochlorite treatment and washed twice with water. The embryo pellet was then flash-frozen in liquid nitrogen and stored at −80 °C before lipid analysis. For *pod-2* and *fasn-1* RNAi treatment, the semisynchronized offspring were allowed to develop for 48 h on empty vector plates to avoid larval arrest and were then washed with M9 buffer and moved to *pod-2* or *fasn-1* RNAi plates for 24 h before embryo collection.

Malonyl-CoA restriction plates

To restrict dietary malonyl-CoA or malonic acid, we used the *E. coli* K12-derived strain L8. The L8 strain contains a temperature-sensitive mutation in the acetyl-CoA carboxylase β-sub-

unit gene, *accB22* (54). The L8 strain normally grows at 30 °C but does not grow above 37 °C due to inhibited malonyl-CoA synthesis. For our feeding experiments, we grew overnight cultures of L8 at 30 °C until the A_{600} of the culture was 2.0. We then collected half of the overnight culture, centrifuged, and concentrated 10× in M9 buffer; plated 300 μl of the bacterial suspension on nutrient-free plates (control); and exposed it to 15 min of UV light in a cell culture hood to prevent further growth. The remaining culture was incubated for an additional 6 h at 40 °C before plating (malonyl-CoA–restricted). Nutrient-free plates contained 1.5% agarose, 50 mM NaCl, 1 mM $CaCl_2$, 1 mM $MgSO_4$, and 25 mM KPO_4.

Biotin, malonyl-CoA, malonic acid, and fatty acid supplementation

Biotin (Sigma-Aldrich, B4501) was dissolved in water at 22 mg/100 ml and filter-sterilized before top-dressing directly onto bacterial feeding plates at 0.05–50 μg/plate. We found that 0.5 μg/plate was sufficient to rescue growth of worms grown on an ACC-restricted diet. Malonic acid (Sigma-Aldrich, M1296) and malonyl-CoA lithium salt (Sigma-Aldrich, M4263) were dissolved in water at 100 mg/ml and then added to the top of bacterial lawns in concentrations ranging from 1 to 200 μg/plate for malonyl-CoA and up to 1000 μg/plate for malonic acid. The 1000-μg/plate replicates caused toxicity and growth arrest of nematodes, which was alleviated by adding NaOH solution to correct the pH; however, no rescue of embryo lethality of *bpl-1(b281)* was observed. Individual fatty acid sodium salts (Nu-Check Prep, Elysian, MN) dissolved in water were added to NGM at 0.1 mM with 0.1% Tergitol before plating as described previously (55).

Author contributions—J. S. W. conducted most of the experiments and wrote most of the paper. D. G. M. and K. J. K. isolated the *bpl-1* mutant strains. D. G. M. performed the mapping and complementation tests and carried out the embryonic phenotype characterization shown in Fig. 1, including filming of the movies. J. S. W., D. G. M., K. J. K., and J. L. W. conceived ideas for the experiments. D. G. M., K. J. K., and J. L. W. edited the paper.

Acknowledgments—Bacterial strains were provided by the Coli Genetic Stock Center, supported by National Science Foundation/Biological Infrastructure/Living Collections program Grant DBI-0742708. Nematode strains were provided by the Caenorhabditis Genetics Center, funded by National Institutes of Health Office of Research Infrastructure Programs Grant P40 OD010440. We thank Liam Coyne for assistance with early bpl-1 RNAi experiments.

References

1. Zempleni, J., Liu, D., Camara, D. T., and Cordonier, E. L. (2014) Novel roles of holocarboxylase synthetase in gene regulation and intermediary metabolism. *Nutr. Rev.* **72,** 369–376 CrossRef Medline
2. Mock, D. M. (2009) Marginal biotin deficiency is common in normal human pregnancy and is highly teratogenic in mice. *J. Nutr.* **139,** 154–157 Medline
3. Sternicki, L. M., Wegener, K. L., Bruning, J. B., Booker, G. W., and Polyak, S. W. (2017) Mechanisms governing precise protein biotinylation. *Trends Biochem. Sci.* **42,** 383–394 CrossRef Medline
4. Rios-Avila, L., Prince, S. A., Wijeratne, S. S., and Zempleni, J. (2011) A 96-well plate assay for high-throughput analysis of holocarboxylase synthetase activity. *Clin. Chim. Acta* **412,** 735–739 CrossRef Medline
5. Wolf, B., Hsia, Y. E., Sweetman, L., Feldman, G., Boychuk, R. B., Bart, R. D., Crowell, D. H., Di Mauro, R. M., and Nyhan, W. L. (1981) Multiple carboxylase deficiency: clinical and biochemical improvement following neonatal biotin treatment. *Pediatrics* **68,** 113–118 Medline
6. Suzuki, Y., Yang, X., Aoki, Y., Kure, S., and Matsubara, Y. (2005) Mutations in the holocarboxylase synthetase gene HLCS. *Hum. Mutat.* **26,** 285–290 CrossRef Medline
7. Kemphues, K. J., Kusch, M., and Wolf, N. (1988) Maternal-effect lethal mutations on linkage group II of *Caenorhabditis elegans*. *Genetics* **120,** 977–986 Medline
8. Reche, P. A. (2000) Lipoylating and biotinylating enzymes contain a homologous catalytic module. *Protein Sci.* **9,** 1922–1929 CrossRef Medline
9. Yang, X., Aoki, Y., Li, X., Sakamoto, O., Hiratsuka, M., Kure, S., Taheri, S., Christensen, E., Inui, K., Kubota, M., Ohira, M., Ohki, M., Kudoh, J., Kawasaki, K., Shibuya, K., Shintani, A., Asakawa, S., Minoshima, S., Shimizu, N., Narisawa, K., Matsubara, Y., and Suzuki, Y. (2001) Structure of human holocarboxylase synthetase gene and mutation spectrum of holocarboxylase synthetase deficiency. *Hum. Genet.* **109,** 526–534 CrossRef Medline
10. Rose, L., and Gonczy, P. (Dec 30, 2014) Polarity establishment, asymmetric division and segregation of fate determinants in early *C. elegans* embryos. *WormBook* 10.1895/wormbook.1.30.2
11. Chandler, R. J., Aswani, V., Tsai, M. S., Falk, M., Wehrli, N., Stabler, S., Allen, R., Sedensky, M., Kazazian, H. H., and Venditti, C. P. (2006) Propionyl-CoA and adenosylcobalamin metabolism in *Caenorhabditis elegans*: evidence for a role of methylmalonyl-CoA epimerase in intermediary metabolism. *Mol. Genet. Metab.* **89,** 64–73 CrossRef Medline
12. Rappleye, C. A., Tagawa, A., Le Bot, N., Ahringer, J., and Aroian, R. V. (2003) Involvement of fatty acid pathways and cortical interaction of the pronuclear complex in *Caenorhabditis elegans* embryonic polarity. *BMC Dev. Biol.* **3,** 8 CrossRef Medline
13. Tagawa, A., Rappleye, C. A., and Aroian, R. V. (2001) Pod-2, along with pod-1, defines a new class of genes required for polarity in the early *Caenorhabditis elegans* embryo. *Dev. Biol.* **233,** 412–424 CrossRef Medline
14. Yi, X., and Maeda, N. (2005) Endogenous production of lipoic acid is essential for mouse development. *Mol. Cell. Biol.* **25,** 8387–8392 CrossRef Medline
15. Gurvitz, A. (2009) A *C. elegans* model for mitochondrial fatty acid synthase II: the longevity-associated gene W09H1.5/mecr-1 encodes a 2-trans-enoyl-thioester reductase. *PLoS One* **4,** e7791 CrossRef Medline
16. Perez, C. L., and Van Gilst, M. R. (2008) A ^{13}C isotope labeling strategy reveals the influence of insulin signaling on lipogenesis in *C. elegans*. *Cell Metab.* **8,** 266–274 CrossRef Medline
17. Dancy, B. C., Chen, S. W., Drechsler, R., Gafken, P. R., and Olsen, C. P. (2015) ^{13}C- and ^{15}N-labeling strategies combined with mass spectrometry comprehensively quantify phospholipid dynamics in *C. elegans*. *PLoS One* **10,** e0141850 CrossRef Medline
18. Watts, J. L., and Browse, J. (2002) Genetic dissection of polyunsaturated fatty acid synthesis in *Caenorhabditis elegans*. *Proc. Natl. Acad. Sci. U.S.A.* **99,** 5854–5859 CrossRef Medline
19. Brooks, K. K., Liang, B., and Watts, J. L. (2009) The influence of bacterial diet on fat storage in *C. elegans*. *PLoS One* **4,** e7545 CrossRef Medline
20. Tanaka, T., Ikita, K., Ashida, T., Motoyama, Y., Yamaguchi, Y., and Satouchi, K. (1996) Effects of growth temperature on the fatty acid composition of the free-living nematode *Caenorhabditis elegans*. *Lipids* **31,** 1173–1178 CrossRef Medline
21. Shi, X., Li, J., Zou, X., Greggain, J., Rødkaer, S. V., Faergeman, N. J., Liang, B., and Watts, J. L. (2013) Regulation of lipid droplet size and phospholipid composition by stearoyl-CoA desaturase. *J. Lipid Res.* **54,** 2504–2514 CrossRef Medline
22. Brock, T. J., Browse, J., and Watts, J. L. (2006) Genetic regulation of unsaturated fatty acid composition in *C. elegans*. *PLoS Genet.* **2,** e108 CrossRef Medline

23. Watts, J. L., and Browse, J. (2000) A palmitoyl-CoA-specific Δ9 fatty acid desaturase from *Caenorhabditis elegans*. *Biochem. Biophys. Res. Commun.* **272,** 263–269 CrossRef Medline
24. Brock, T. J., Browse, J., and Watts, J. L. (2007) Fatty acid desaturation and the regulation of adiposity in *Caenorhabditis elegans*. *Genetics* **176,** 865–875 Medline
25. Benenati, G., Penkov, S., Müller-Reichert, T., Entchev, E. V., and Kurzchalia, T. V. (2009) Two cytochrome P450s in *Caenorhabditis elegans* are essential for the organization of eggshell, correct execution of meiosis and the polarization of embryo. *Mech. Dev.* **126,** 382–393 CrossRef Medline
26. Olson, S. K., Greenan, G., Desai, A., Muller-Reichert, T., and Oegema, K. (2012) Hierarchical assembly of the eggshell and permeability barrier in *C. elegans*. *J. Cell Biol.* **198,** 731–748 CrossRef Medline
27. Zhu, H., Shen, H., Sewell, A. K., Kniazeva, M., and Han, M. (2013) A novel sphingolipid-TORC1 pathway critically promotes postembryonic development in *Caenorhabditis elegans*. *Elife* **2,** e00429 Medline
28. Zhang, H., Abraham, N., Khan, L. A., Hall, D. H., Fleming, J. T., and Göbel, V. (2011) Apicobasal domain identities of expanding tubular membranes depend on glycosphingolipid biosynthesis. *Nat. Cell Biol.* **13,** 1189–1201 CrossRef Medline
29. Takamura, Y., and Nomura, G. (1988) Changes in the intracellular concentration of acetyl-CoA and malonyl-CoA in relation to the carbon and energy metabolism of *Escherichia coli* K12. *J. Gen. Microbiol.* **134,** 2249–2253 Medline
30. Hirsh, D., Oppenheim, D., and Klass, M. (1976) Development of the reproductive system of *Caenorhabditis elegans*. *Dev. Biol.* **49,** 200–219 CrossRef Medline
31. Tang, H., and Han, M. (2017) Fatty acids regulate germline sex determination through ACS-4-dependent myristoylation. *Cell* **169,** 457–469.e13 CrossRef Medline
32. Watson, E., MacNeil, L. T., Ritter, A. D., Yilmaz, L. S., Rosebrock, A. P., Caudy, A. A., and Walhout, A. J. (2014) Interspecies systems biology uncovers metabolites affecting *C. elegans* gene expression and life history traits. *Cell* **156,** 759–770 CrossRef Medline
33. Watson, E., Olin-Sandoval, V., Hoy, M. J., Li, C. H., Louisse, T., Yao, V., Mori, A., Holdorf, A. D., Troyanskaya, O. G., Ralser, M., and Walhout, A. J. (2016) Metabolic network rewiring of propionate flux compensates vitamin B12 deficiency in *C. elegans*. *Elife* **5,** e17670 CrossRef Medline
34. Lin, C. J., and Wang, M. C. (2017) Microbial metabolites regulate host lipid metabolism through NR5A-Hedgehog signalling. *Nat. Cell Biol.* **19,** 550–557 CrossRef Medline
35. Uchida, Y., and Holleran, W. M. (2008) *ω-O*-acylceramide, a lipid essential for mammalian survival. *J. Dermatol. Sci.* **51,** 77–87 CrossRef Medline
36. Zheng, Y., Yin, H., Boeglin, W. E., Elias, P. M., Crumrine, D., Beier, D. R., and Brash, A. R. (2011) Lipoxygenases mediate the effect of essential fatty acid in skin barrier formation: a proposed role in releasing *ω*-hydroxyceramide for construction of the corneocyte lipid envelope. *J. Biol. Chem.* **286,** 24046–24056 CrossRef Medline
37. Burri, B. J., Sweetman, L., and Nyhan, W. L. (1981) Mutant holocarboxylase synthetase: evidence for the enzyme defect in early infantile biotin-responsive multiple carboxylase deficiency. *J. Clin. Invest.* **68,** 1491–1495 CrossRef Medline
38. Moore, J. H., and Christie, W. W. (1979) Lipid metabolism in the mammary gland of ruminant animals. *Prog. Lipid Res.* **17,** 347–395 CrossRef Medline
39. Post-Beittenmiller, D., Roughan, G., and Ohlrogge, J. B. (1992) Regulation of plant fatty acid biosynthesis: analysis of acyl-coenzyme a and acyl-acyl carrier protein substrate pools in spinach and pea chloroplasts. *Plant Physiol.* **100,** 923–930 CrossRef Medline
40. McGarry, J. D., Leatherman, G. F., and Foster, D. W. (1978) Carnitine palmitoyltransferase I: the site of inhibition of hepatic fatty acid oxidation by malonyl-CoA. *J. Biol. Chem.* **253,** 4128–4136 Medline
41. McGarry, J. D., Mannaerts, G. P., and Foster, D. W. (1977) A possible role for malonyl-CoA in the regulation of hepatic fatty acid oxidation and ketogenesis. *J. Clin. Invest.* **60,** 265–270 CrossRef Medline
42. Bao, B., Wijeratne, S. S. K., Rodriguez-Melendez, R., and Zempleni, J. (2011) Human holocarboxylase synthetase with a start site at methionine-58 is the predominant nuclear variant of this protein and has catalytic activity. *Biochem. Biophys. Res. Commun.* **412,** 115–120 CrossRef Medline
43. Narang, M. A., Dumas, R., Ayer, L. M., and Gravel, R. A. (2004) Reduced histone biotinylation in multiple carboxylase deficiency patients: a nuclear role for holocarboxylase synthetase. *Hum. Mol. Genet.* **13,** 15–23 Medline
44. Trujillo-Gonzalez, I., Cervantes-Roldan, R., Gonzalez-Noriega, A., Michalak, C., Reyes-Carmona, S., Barrios-Garcia, T., Meneses-Morales, I., and Leon-Del-Rio, A. (2014) Holocarboxylase synthetase acts as a biotin-independent transcriptional repressor interacting with HDAC1, HDAC2 and HDAC7. *Mol. Genet. Metab.* **111,** 321–330 CrossRef Medline
45. Stiernagle, T. (2006) Maintenance of *C. elegans* (February 11, 2006) *WormBook* (The *C. elegans* Research Community, ed) CrossRef
46. Mello, C. C., Kramer, J. M., Stinchcomb, D., and Ambros, V. (1991) Efficient gene transfer in *C. elegans*: extrachromosomal maintenance and integration of transforming sequences. *EMBO J.* **10,** 3959–3970 Medline
47. Fraser, A. G., Kamath, R. S., Zipperlen, P., Martinez-Campos, M., Sohrmann, M., and Ahringer, J. (2000) Functional genomic analysis of *C. elegans* chromosome I by systematic RNA interference. *Nature* **408,** 325–330 CrossRef Medline
48. Verbrugghe, K. J., and Chan, R. C. (2011) Imaging C. elegans embryos using an epifluorescent microscope and open source software. *J. Vis. Exp.* CrossRef Medline
49. Rappleye, C. A., Tagawa, A., Lyczak, R., Bowerman, B., and Aroian, R. V. (2002) The anaphase-promoting complex and separin are required for embryonic anterior-posterior axis formation. *Dev. Cell* **2,** 195–206 CrossRef Medline
50. Brennan, L. D., Roland, T., Morton, D. G., Fellman, S. M., Chung, S., Soltani, M., Kevek, J. W., McEuen, P. M., Kemphues, K. J., and Wang, M. D. (2013) Small molecule injection into single-cell *C. elegans* embryos via carbon-reinforced nanopipettes. *PLoS One* **8,** e75712 CrossRef Medline
51. Boyd, L., Guo, S., Levitan, D., Stinchcomb, D. T., and Kemphues, K. J. (1996) PAR-2 is asymmetrically distributed and promotes association of P granules and PAR-1 with the cortex in *C. elegans* embryos. *Development* **122,** 3075–3084 Medline
52. Etemad-Moghadam, B., Guo, S., and Kemphues, K. J. (1995) Asymmetrically distributed PAR-3 protein contributes to cell polarity and spindle alignment in early *C. elegans* embryos. *Cell* **83,** 743–752 CrossRef Medline
53. Robert, V. J., Sijen, T., van Wolfswinkel, J., and Plasterk, R. H. (2005) Chromatin and RNAi factors protect the *C. elegans* germline against repetitive sequences. *Genes Dev.* **19,** 782–787 CrossRef Medline
54. Harder, M. E., Beacham, I. R., Cronan, J. E., Jr., Beacham, K., Honegger, J. L., and Silbert, D. F. (1972) Temperature-sensitive mutants of *Escherichia coli* requiring saturated and unsaturated fatty acids for growth: isolation and properties. *Proc. Natl. Acad. Sci. U.S.A.* **69,** 3105–3109 CrossRef Medline
55. Deline, M. L., Vrablik, T. L., and Watts, J. L. (2013) Dietary supplementation of polyunsaturated fatty acids in *Caenorhabditis elegans*. *J. Vis. Exp.* CrossRef Medline